A Demonstration Of The Theory Of Spatial Repeatability

Tom Moran
PACCAR Technical Center, USA

Margaret Sullivan
Kenworth Truck Company, USA

Joe Mahoney
Washington State Transportation Center, University of Washington, USA

Karim Chatti
Department of Civil and Environmental Engineering, Michigan State University, USA

ABSTRACT

A heavy vehicle/pavement test was conducted at the PACCAR Technical Center to demonstrate the theory of spatial repeatability and to quantify the pavement strain levels caused by heavy vehicle dynamic wheel loads.

Six test vehicles consisting of four tractor semi-trailers and two trucks were repeatedly driven over a ramp designed to excite the rigid body (sprung mass) vibration modes. Pavement strain responses were measured using a strain gaged section of asphalt concrete.

Pavement strain gage responses showed consistent and repeatable areas of high versus low strains for this group of test vehicles. In addition, the magnitudes of these measured pavement strains were high enough to be potentially damaging to the pavement.

INTRODUCTION

It has been widely recognized by both pavement and vehicle engineers that heavy trucks play a major role regarding road damage in the US and Canada. Technical professionals from the PACCAR Technical Center have been members of a team of research scientists and engineers studying the interactions between heavy trucks and pavements since 1988. This research team included members from industry, government, and universities. Represented institutions included the PACCAR Technical Center, the University of Washington, Washington State University, Michigan State University, the University of California at Berkeley, and the Washington State Department of Transportation.

It has been PACCAR's mission to join with researchers from the pavement community and work towards the goal of enhancing the overall efficiency of the highway/vehicle transportation system. PACCAR's contribution to this effort to date has been to: 1) provide a strain gaged section of flexible pavement at the PACCAR Technical Center to study pavement/heavy truck interactions and validate pavement models, 2) provide test vehicles, personnel, and equipment for pavement strain measurement tests, and 3) provide heavy truck engineering and testing expertise for the research team in interpreting the test data.

PURPOSE AND SCOPE

There has been published evidence from researchers suggesting that dynamic wheel loads induced by a variety of different vehicles are repetitive along the same points for a given road (Gyenes, 1992) and will result in greater degrees of damage for certain sections of the road. The term "spatial repeatability" has been used to label or refer to this phenomenon.

In addition, past research also suggests that the magnitudes of these spatially repetitive dynamic wheel loads are sufficient to significantly decrease the pavement fatigue life (Gillespie, 1992; Potter 1994).

In addition to the joint research on heavy truck and pavement interactions referred to in the introduction, PACCAR has been conducting research directed towards the goal of developing "road-friendly" trucks through the reduction of dynamic wheel loads.

A major part of this effort has been to develop a test methodology utilizing a road simulator for generating realistic dynamic wheel loads in the test laboratory (Moran, Sullivan, Menmuir, Mahoney, 1995). However, in order to justify the resources needed to develop the road simulator into a tool for developing "road friendly" heavy trucks, it was deemed necessary to first demonstrate that dynamic wheel loads were a major factor influencing pavement service life. To accomplish this task, a test was performed at the PACCAR Technical Center to measure the strain levels in a section of strain-gaged asphalt pavement resulting from the dynamic wheel loads caused by a sample of heavy trucks and to demonstrate the theory of spatial repeatability. The purpose of this paper is to document the results of the dynamic wheel load testing of PACCAR's asphalt pavement.

The scope of this test was limited to: 1) a sample of 6 vehicles with different rear suspensions, 2) a 40 ft. strain gaged section of track with the gages mounted at 1 ft. intervals, and 3) an excitation bump designed to excite only the low frequency rigid body modes of the vehicles.

METHODOLOGY

TEST VEHICLES

Six test vehicles were used during this test. Two class 8 tractors and 2 semi-trailers were interchanged to account for 4 of the test vehicles. The 2 remaining vehicles were configured as trucks. The wheelbases for these trucks and tractors were intentionally chosen to be similar in order to better isolate the contributions of the different suspensions to the pavement strain profiles. All test vehicle were loaded near their legal limits and tire pressures were set to the rated maximums. One of these trucks, a Peterbilt 359 had strain gaged axles (bending bridge configuration) and wheel end accelerometers for measuring dynamic wheel loads as had been done in previous studies (Cebon, 1993). Table 1 contains descriptions of the test vehicles. Figures 1 through 4 present photographs of the test vehicles.

Table 1. Test vehicles

Vehicle	Make/Model	Wheelbase or Length	Rear Suspension
Tractor 1	Kenworth T600A	225 in.	Tandem 8 bag air
Tractor 2	Kenworth T800	236 in.	Tandem walking beam
Trailer 1	Fruehauf Van	48 ft.	Tandem 4 spring
Trailer 2	Aztec Flatbed	40 ft.	Tandem 4 spring
Truck 1	Peterbilt 359	225 in.	Tandem 4 spring
Truck 2	Peterbilt 330	245 in.	Single leaf spring

Figure 1. Kenworth T600A

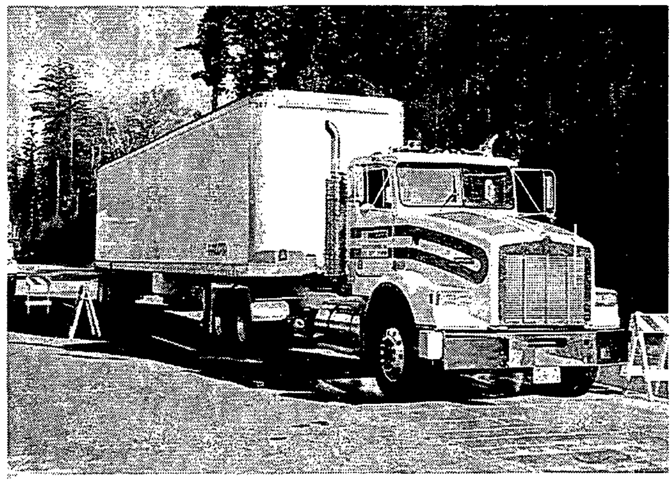

Figure 2. Kenworth T800A with Fruehauf trailer

Figure 3. Peterbilt 359

Figure 4. Peterbilt 330

Figure 5. The test ramp

EXCITATION SOURCE

The excitation source was a test ramp designed to excite the rigid body sprung mass modes of the test vehicles and not the unsprung mass modes (i.e. axle hop). This was done to help simplify and analyze the pavement strain response data. The ramp design consisted of a 4 ft by 2 in ramp-up, a 7 ft flat section, and a 4 ft by 2 in ramp-down. Figure 5 presents a photograph of the ramp.

INSTRUMENTED PAVEMENT

The instrumented asphalt pavement section at the PACCAR Technical Center was comprised of 102 foil strain gages. Figure 6 presents a schematic of the instrumented pavement.

Thirty two transverse surface gages mounted in a single row at 1 ft intervals on the east side on the pavement section were used for this test. Detailed information on this instrumented pavement section has been documented in a separate paper (Chatti, Mahoney, Monismith, Moran, 1995).

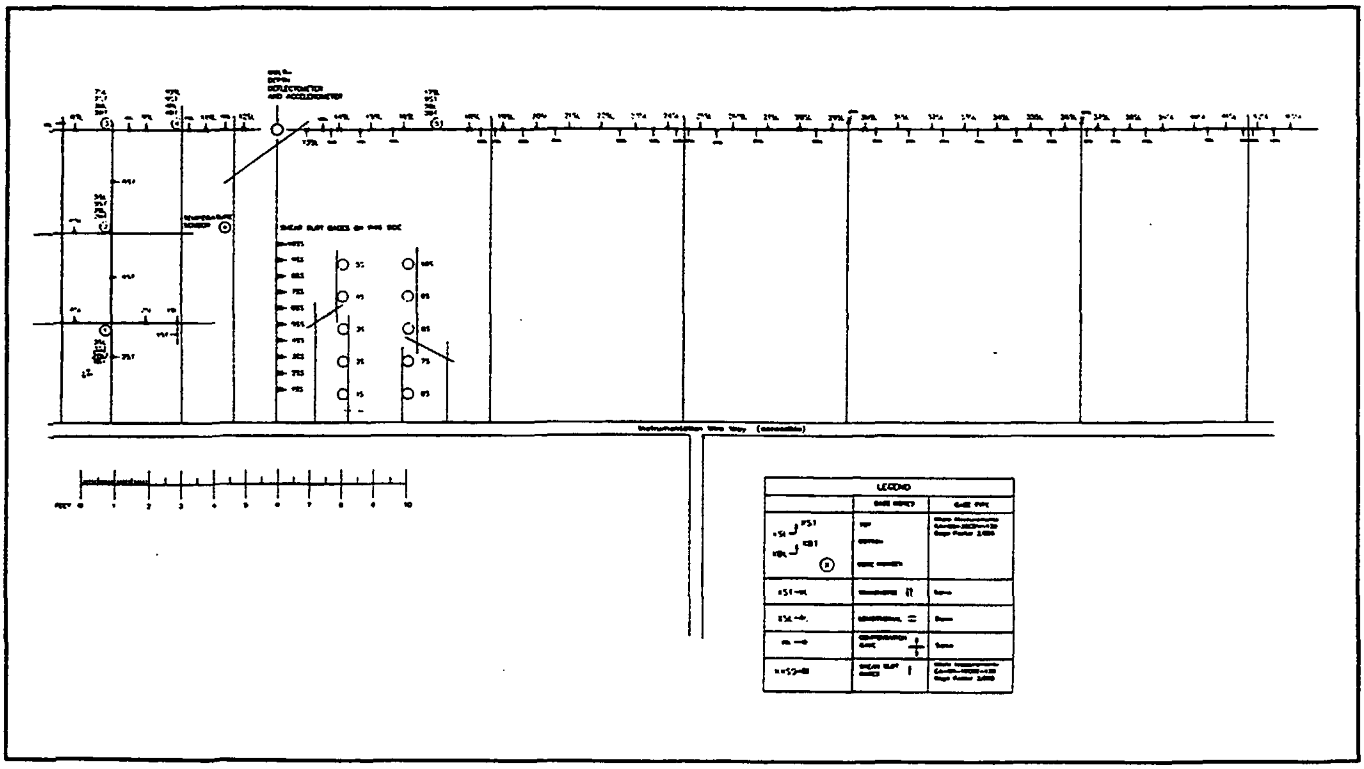

Figure 6. The instrumented pavement section

TEST PROCEDURE

A total of 54 test runs were conducted for the 6 test vehicles (i.e. 9 repeat runs for each test vehicle). The runs were divided into 3 blocks of 18 runs in order to reduce the effects of temperature changes during the day. The order of testing for each vehicle within a given block was randomized.

Note that the Peterbilt 359 was the only test vehicle equipped with instrumentation to measure dynamic wheel loads. This vehicle instrumentation was triggered simultaneously with the pavement gages to allow matching this vehicles wheel load inputs to the pavement strain responses.

Due to the 40 ft length of the instrumented pavement section and the need to obtain at least 2 rigid body vibration cycles at frequencies as low as 2 Hz, vehicle speed was set at 20 mph (29.3 ft/sec) for all test runs.

Since tire placements relative to the pavement gages were critical, lime powder was sprinkled over the gage areas to record the actual location of the tires relative to the gages. In order to maximize the likelihood of adequate tire placements, a row of wide tape was laid parallel to the gage row and sights were fabricated onto the trucks to aid the driver with the task of lining up the truck with the tape. In addition, tire offsets relative to the gage locations were taken at the beginning of the gage row, at the midpoint of the gage row, and at the end of the gage row. Any test runs with tire offsets greater than 4 inches were discarded and repeated. All tire offsets were recorded relative to the outer-most tire on the vehicle. Tire offsets for the other wheels were calculated based on each vehicle's geometry. Figure 7 presents a photograph of the strain gaged pavement during testing.

Figure 7. The instrumented pavement during testing

Pavement temperatures were also measured and recorded immediately after each test run.

DATA ANALYSIS

For each test run, the peak strain values for every pavement gage were matched to the responsible test vehicle wheel. These strain levels were also adjusted for wheel location offsets relative to the gage and for surface temperature variations based on layered elastic theory and laboratory measured asphalt-concrete moduli.

Outer-most wheel offsets at each gage location were calculated from the 3 measured wheel offsets (i.e. the beginning, middle, and end of the gage row) and from the test vehicle's wheel location geometry. The strain levels were then proportionally increased (i.e. in percent) to compensate for the wheel not being directly over the gage based on the magnitude and direction of the wheel position offset (outboard or inboard) using the following process.

For dual tires, inboard offset:

$\varepsilon_{\%} = 0\%$:for wheel offset $\leq$ 1 in

$\varepsilon_{\%} = 3.5\,(\text{offset} - 1)$:for wheel offset > 1 in and $\leq$ 4 in

For dual tires, outboard offset:

$\varepsilon_{\%} = 5.8\,(\text{offset})$:for wheel offset $\leq$ 4 in

For single tires:

$\varepsilon_{\%} = 3.0 + 12.0\,(\text{abs(offset)} - 1)$:for wheel offset $\leq$ 4 in

The strain adjustments due to asphalt concrete surface temperature variations were conducted using the following process:

Step 1: Calculated pavement modulus of elasticity based on asphalt concrete temperature as follows:

$$E_{ac} = 10^{(6.4721 - 1.474\times10^{-4}(T^2))}$$

Where: T = temperature (deg F)
E_{ac} = asphalt modulus of elasticity (psi)

Step 2: Referenced all strain measurements to 77 deg F as follows:

If pavement temperature > 77 deg F:

Calculated strain ratio:

$$SR = 1.0 + .049\,(E_{ac77}/E_{acX} - 1)$$

Where: SR = strain ratio
E_{ac77} = 396635 psi
$E_{acX} = E_{ac}$ at actual pavement temperature

The adjusted pavement strain was then calculated by:

$$\varepsilon_{77} = \varepsilon_X (SR)$$

Where: ε_{77} = adjusted strain referenced to 77 deg F
ε_X = measured strain at actual temperature

If pavement temperature $\leq$ 77 deg F, the above steps were followed except the strain ratio equation was changed to:

$$SR = 1.0 + 0.65(E_{acX}/E_{ac77} - 1)$$

Due to the large quantity of data points collected and the extent of the calculation process involved, the data were reduced using a programming language designed for a commercial spreadsheet package. The spreadsheet environment was also ideal for constructing the many graphs needed to interpret the reduced data.

RESULTS

The results of this test are presented in graphical form as described below.

Figure 8 presents a graph of pavement strain versus distance along the gage row for all of the test vehicles. Note the areas of high and low strain which were reasonably consistent for all of the test vehicles.

Figures 9 through 14 present graphs of pavement strain versus distance along the gage row for each test vehicle separately based on wheel location.

Figure 15 presents a graph of the wheel loads from the PB359 versus distance along the gage row based on wheel location.

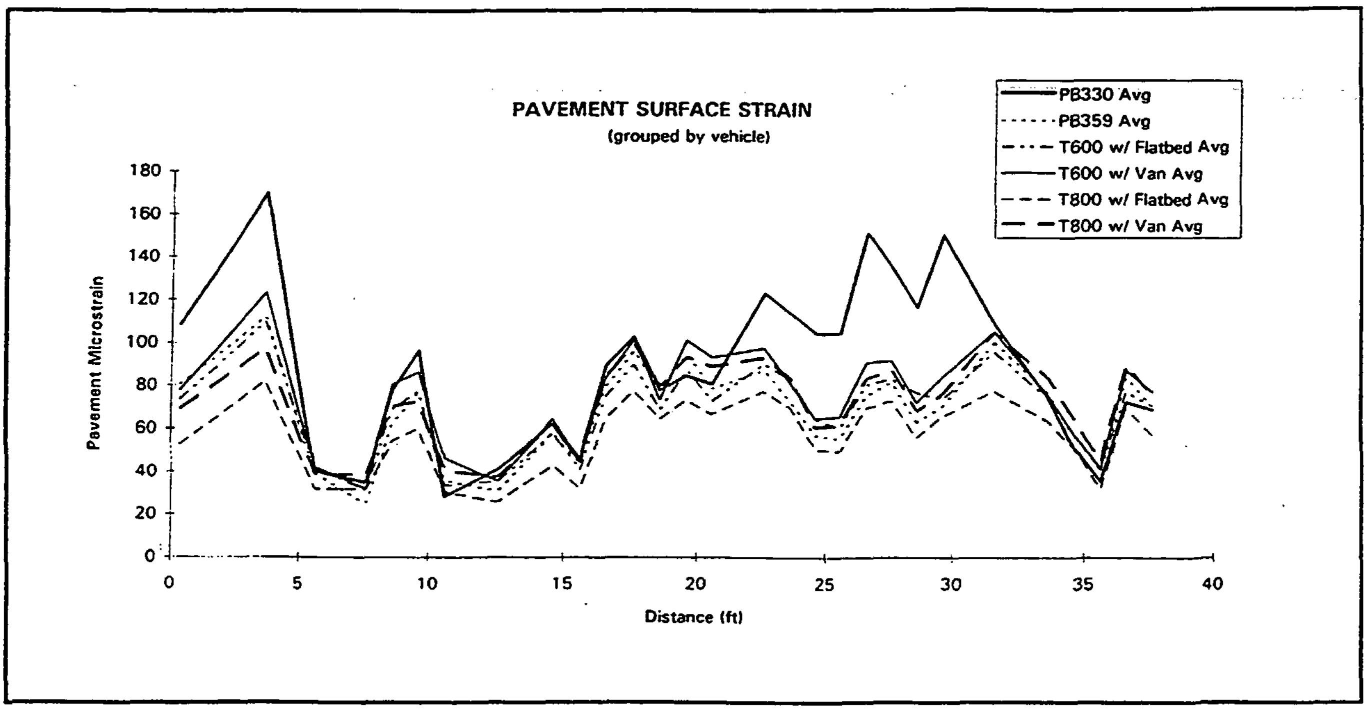

Figure 8. Pavement strain versus position on the pavement based on test vehicle

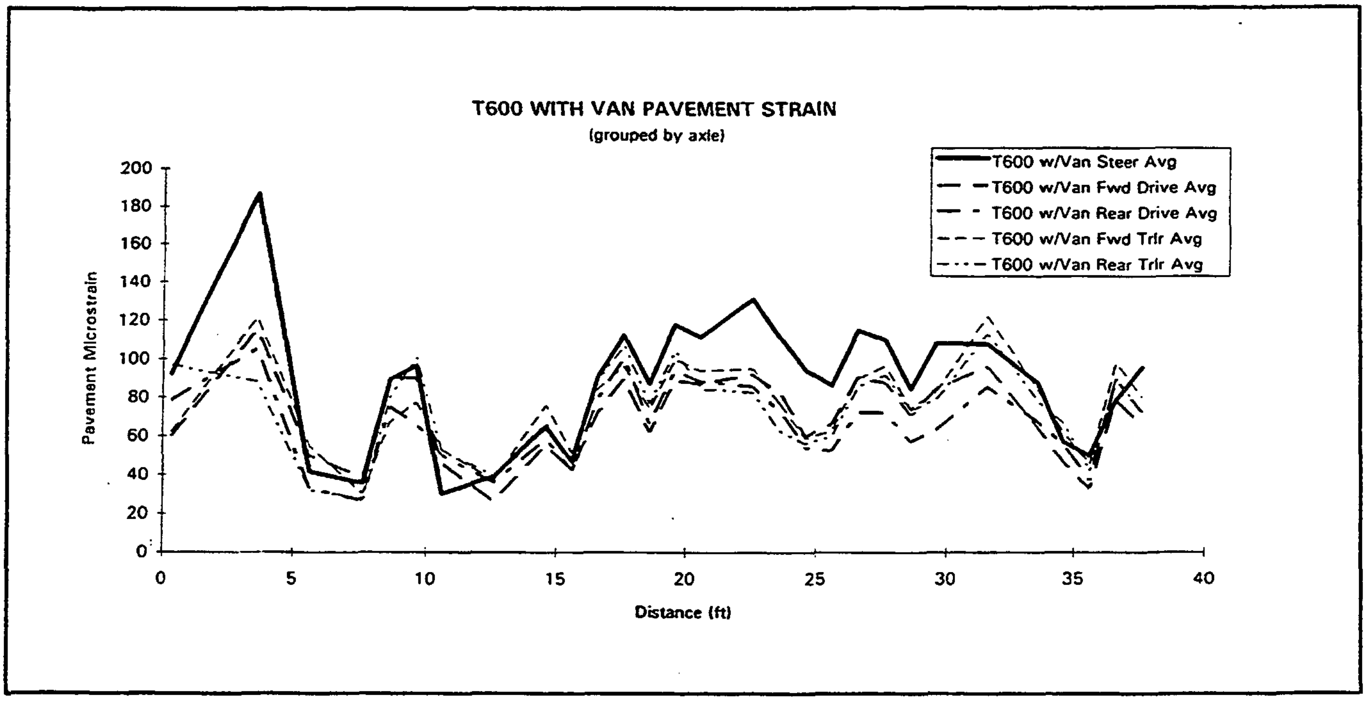

Figure 9. Pavement strain versus position on the pavement based on wheel position for the T600A with van trailer

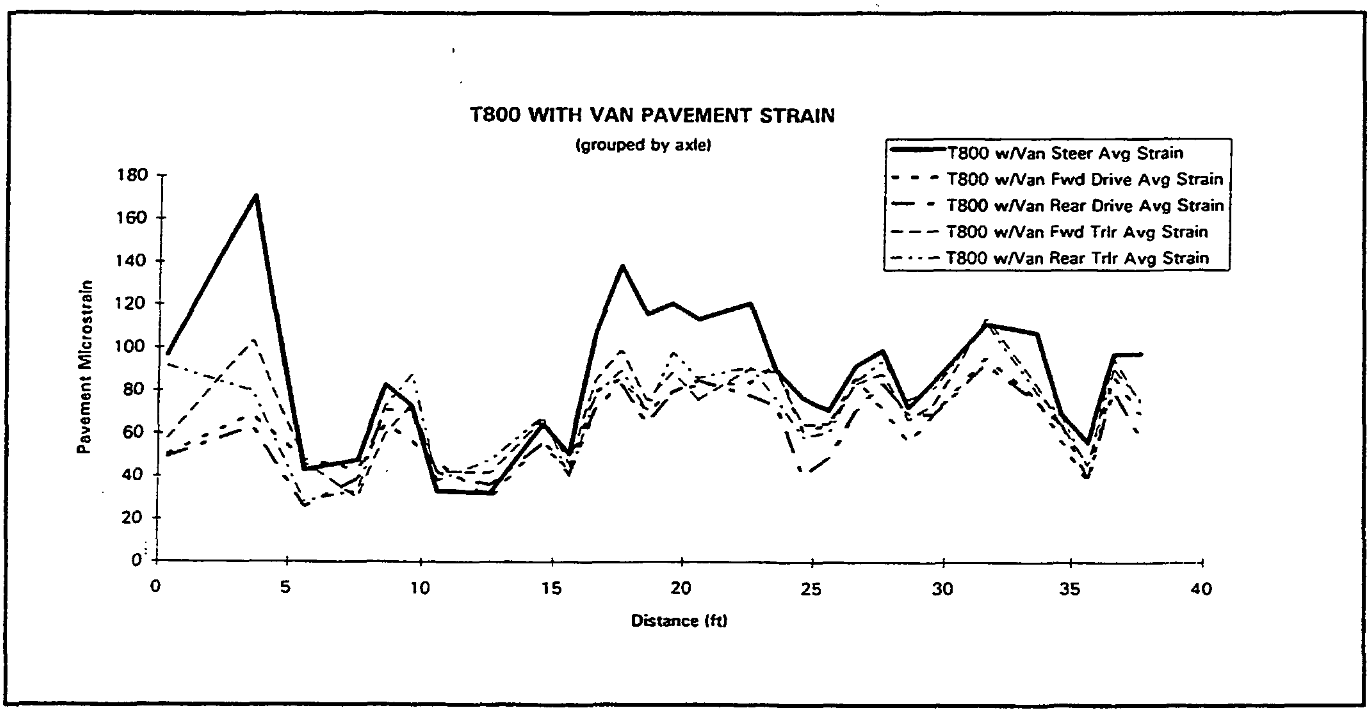

Figure 10. Pavement strain versus position on the pavement based on wheel position for the T800 with van trailer

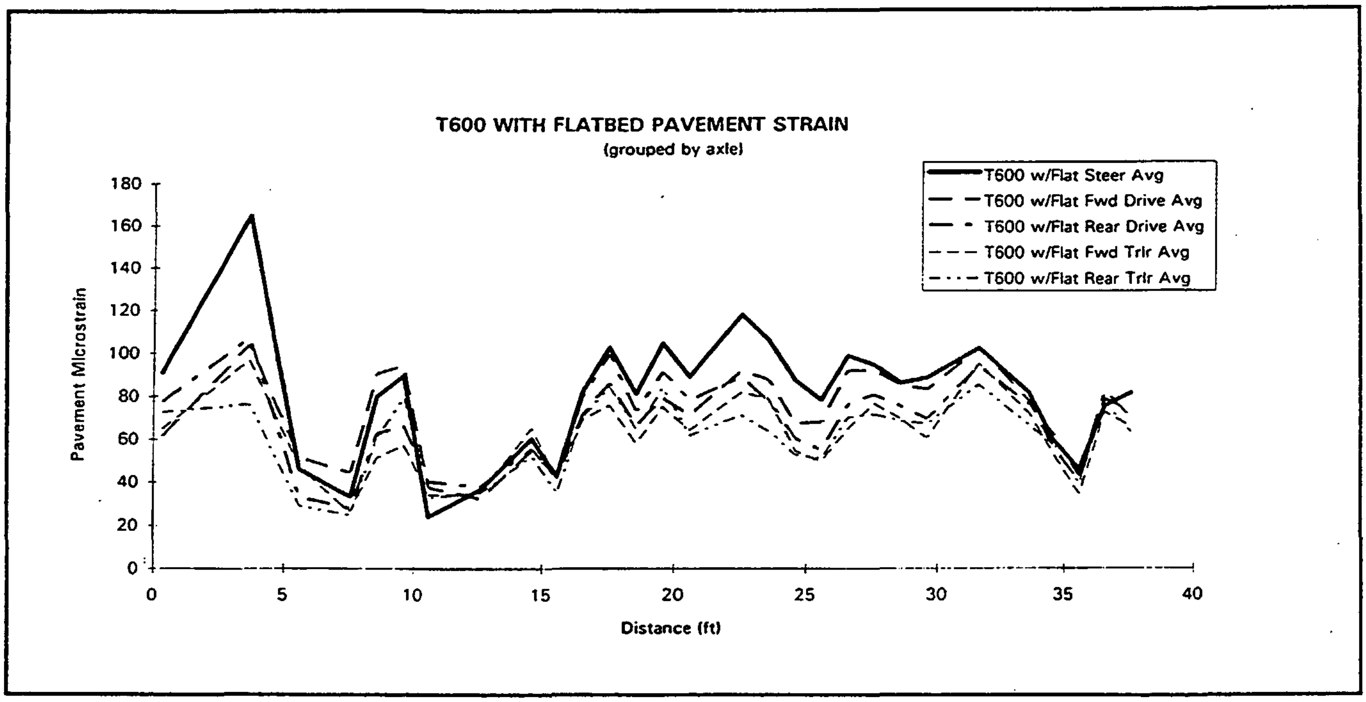

Figure 11. Pavement strain versus position on the pavement based on wheel position for the T600A with flatbed trailer

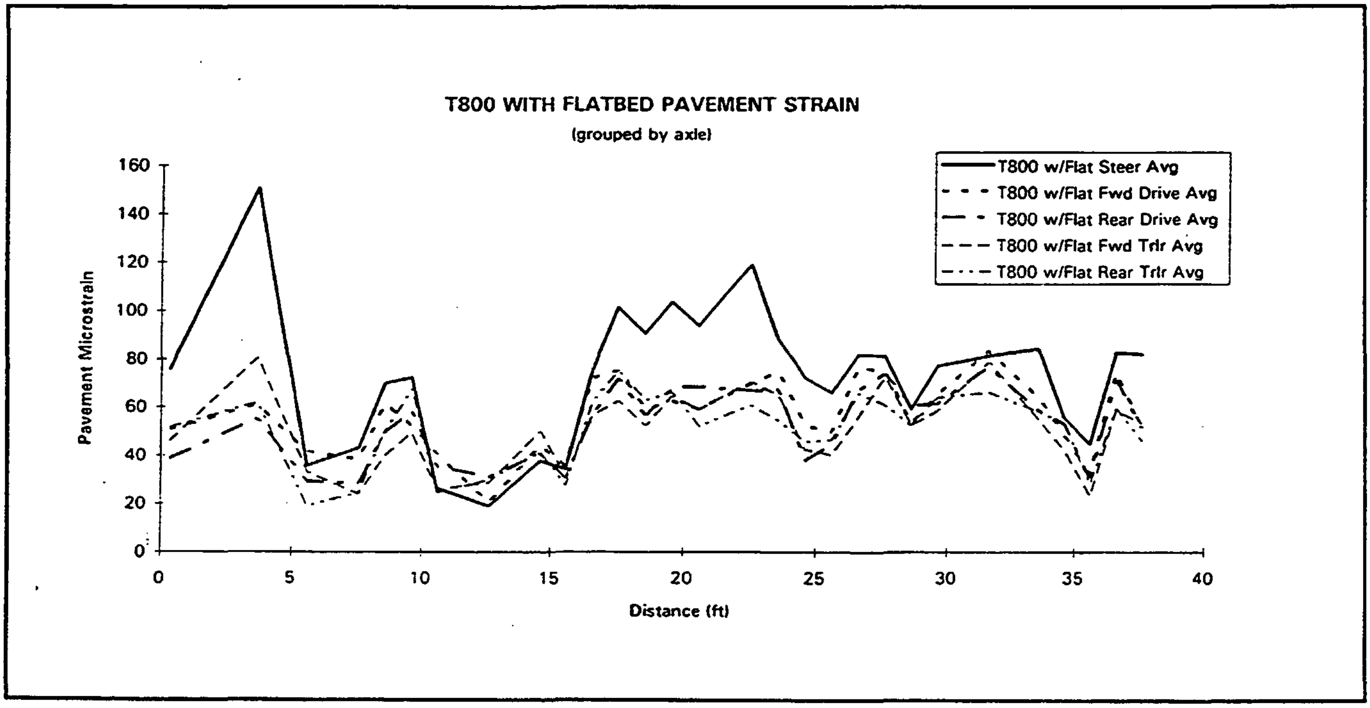

Figure 12. Pavement strain versus position on the pavement based on wheel position for the T800 with flatbed trailer

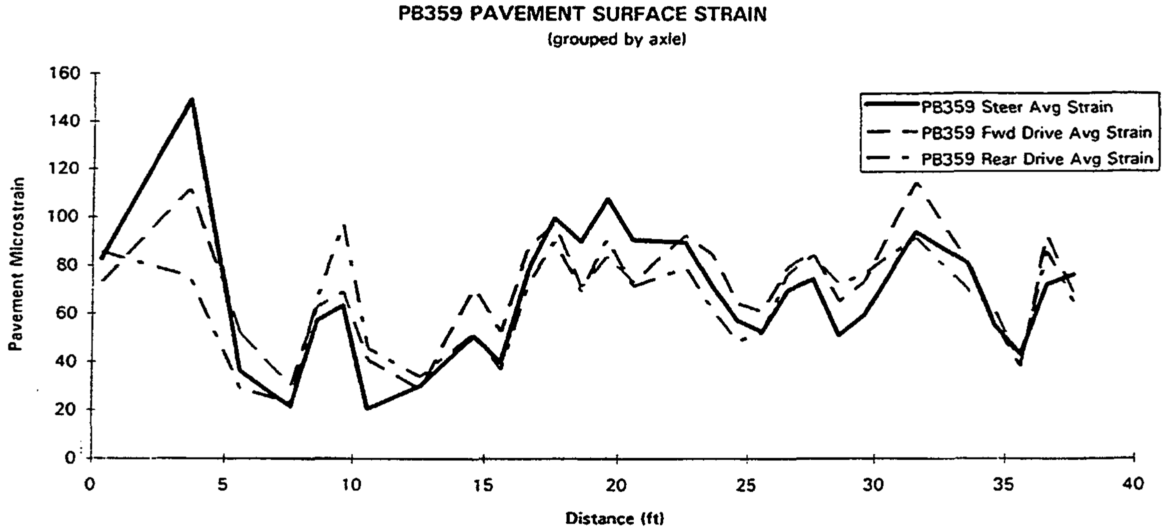

Figure 13. Pavement strain versus position on the pavement based on wheel position for the PB359

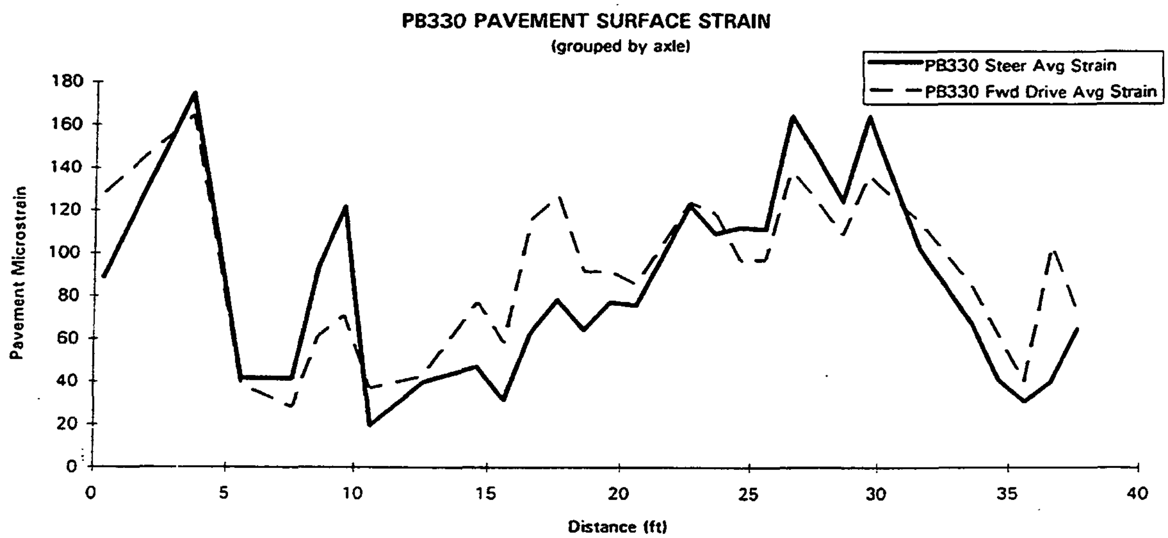

Figure 14. Pavement strain versus position on the pavement based on wheel position for the PB330

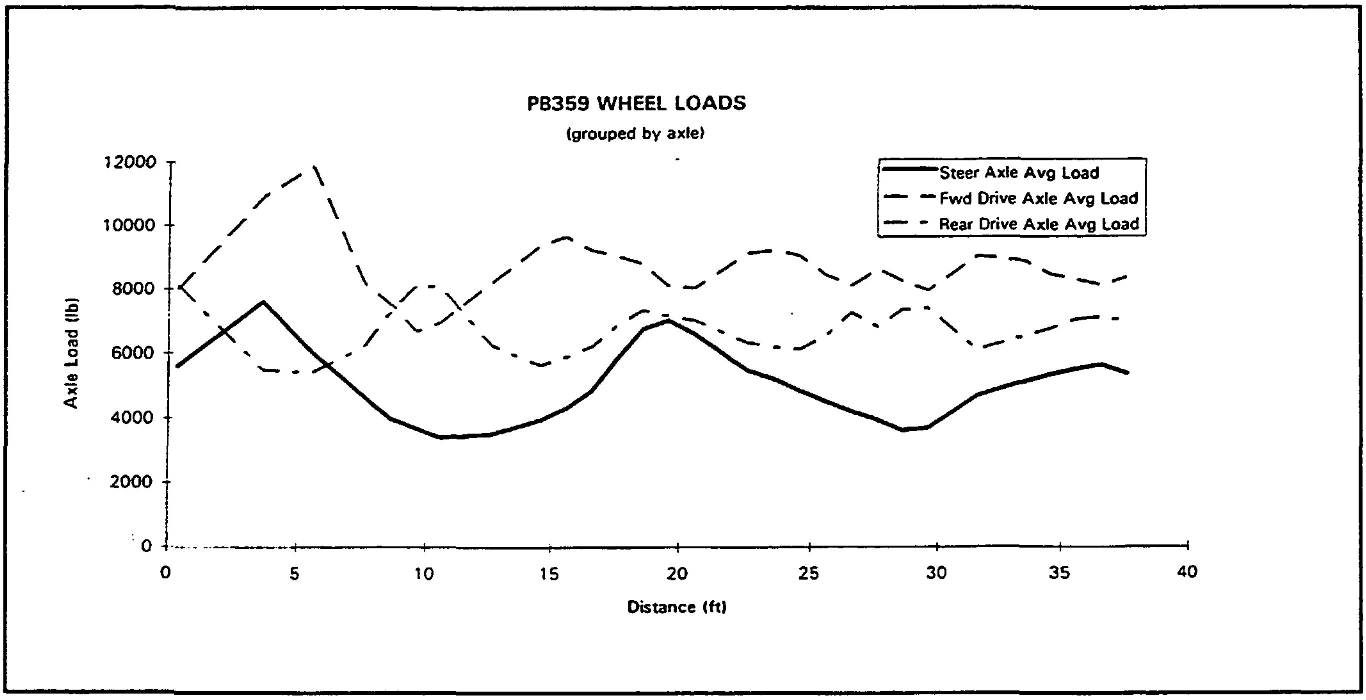

Figure 15. Wheel load versus position on the pavement for the PB359

DISCUSSION OF RESULTS

The results of this testing appear to support the concept of spatial repeatability based on the graph in Figure 8. As seen on this graph there were distinct areas of higher versus lower peak pavement strains which remained consistent for all the vehicles tested. Also, the wheel loads from the PB359 shown in Figure 15 corresponded to this strain pattern.

Also of note, the steer axle tires caused the highest peak pavement strains for all of the test vehicles. This supports previous research results indicating that single tires on the steer axle loaded to 12000 lb. are typically more damaging than the dual tires on drive axles loaded up to 20000 lb. (Gillespie et al, 1992).

Lastly, the effects of suspension type on peak pavement strains was surprising. As can be seen from figures 9 through 12, the peak pavement strains generated by the T600A with 8-airbag rear suspension were higher than those caused by the T800 with walking beam rear suspension.

Note that these vehicles had comparable wheelbases and static axle loads. At first glance this appears to contradict the popular belief that air suspensions are more road-friendly than walking-beam suspensions.

However, it is worth noting that the excitation source in combination with a the constant vehicle speed was designed to excite only the low frequency responses of the test vehicles. From visual observations of the vehicles during testing, it was apparent that the air and leaf spring rear suspensions were compressed at or near the limits of their travel. Therefore, it is possible that the rear air suspension may have contacted the bump-stops. Furthermore, the geometry of the excitation source in combination with the vehicle speed and the vehicle wheelbases could allow the load transfers feature of the walking beam suspension to produce lower dynamic wheel loads at the high strain pavement locations.

Investigations into what actually caused the above surprising suspension dynamic load behavior were beyond the scope of this project and are left to future suspension "road-friendliness" research.

ACKNOWLEDGMENTS

The author thanks Hal Brown, Roy Gravley, Rody Martin, Ken Moller, and Joyce Smith for their professionalism and dedication to this project. Their willingness to put in the extra time and effort necessary to successfully complete this project is very much appreciated.

REFERENCES

Gyenes, L and Mitchell, C. (1992) "The spatial repeatability of dynamic pavement loads caused by heavy goods vehicles", Proceedings of the 3rd International Symposium on Heavy Vehicle Weights and Dimensions, June 1992, Cambridge.

Gillespie, T (1992) "Truck factors affecting dynamic loads and road damage", Heavy vehicles and roads, Proceeding of the 3rd International Symposium on Heavy Vehicle Weights and Dimensions, June 1992, Cambridge

Moran, Sullivan, Menmuir, and Mahoney, (1995) "Replication of heavy truck dynamic wheel loads using a road simulator", Proceeding of the Fourth International Symposium on Heavy Vehicle Weights and Dimension, June 1995.

Potter, T (1994) "Road damage due to dynamic tyre forces measured on a public road", Third engineering foundation conference on vehicle-road and vehicle-bridge interaction, June 1994, Holland.

Cebon, D. (1993) "Interaction between heavy vehicles and roads", Appendix A, pp. 77 - 78, The thirty-ninth L. Ray Buckendale Lecture, Paper 930001, submitted to the Society of Automotive Engineers

Chatti, Mahoney, Monismith, and Moran (1995) "Field response and dynamic modeling of an asphalt concrete pavement section under moving heavy trucks. Proceeding of the Fourth International Symposium on Heavy Vehicle Weights and Dimension, June 1995.

Gillespie, T (1992) "Effects of heavy vehicle characteristics on pavement response and performance", Transportation Research Board, NCHRP Report 1-25(1).